Spectroscopic Study of the Interaction of Anticancer Drug Mitoxantrone with Sodium Cholate Aggregates

MIRELA ENACHE*, ANA MARIA TOADER
Institute of Physical Chemistry Ilie Murgulescu, Romanian Academy, 202 Splaiul Independentei, 060021, Bucharest, Romania

The focus of the present work is to investigate the interaction of anticancer drug mitoxantrone with sodium cholate (NaC) bile salt in phosphate buffer (pH 7.4) and carbonate buffer (pH 10) by UV-Visible absorption spectroscopy. The results indicate that mitoxantrone may bind to NaC monomers and micelles through electrostatic and hydrophobic interactions and the interaction with NaC induces the dissociation of dimers and higher aggregates of mitoxantrone. The stoichiometric ratio, binding constant, micelle/water partition coefficient and the corresponding thermodynamic parameters for binding and partitioning processes were estimated from the monomer absorbance changes occurred as a result of the interaction between mitoxantrone and NaC micelles. The binding process of mitoxantrone to NaC micelles is spontaneous and entropy controlled over the range of studied temperatures, at both pH values. The partition process of mitoxantrone between micellar and bulk aqueous phases is spontaneous and entropy controlled at pH 7.4 but enthalpy controlled at pH 10.

Keywords: mitoxantrone, bile salts, micelles, binding constant, partition coefficient

Bile salts are naturally occurring amphiphiles which are produced in liver and are involved in different biological functions, such as digestion and adsorption of lipids and cholesterol in the small intestine [1, 2]. Bile salts with the advantage of physiological compatibility are used in the formulation of food and cosmetics, and in clinical medicine for enhancing drug solubility and improving the adsorption and bioavailability [3, 4]. The structure of bile salt is very different from that of conventional surfactants. Bile salts have a core comprising a large, rigid, and hydrophobic steroid moiety with attached hydrophilic groups (two or three hydroxyl groups) and an anionic carboxyl head group. Bile salts thus have a facial structure with a hydrophobic side and a hydrophilic side or, depending on the position and orientation of the hydroxyl groups, a hydrophilic edge only. The hydrophobic and hydrophilic domains are not clearly separated as in classical surfactants [5]. Due to the presence of two different binding sites, bile salt micelles were suggested to be suitable for carrying both hydrophilic and hydrophobic molecules depending on the structure and size of the molecules [6-9]. As a result of the structure, the aggregation behaviour and the shape of the micelles of the bile salts are different from those of common surfactants [5]. Different models have been proposed to explain the unusual aggregation process of bile salts. The most accepted model known as Small's model is a two-step model with the formation of primary and secondary micelles [10-12]. According to this model, the primary micelles with hydrophobic binding sites are formed at lower bile salt concentration by the hydrophobic interaction between the hydrophobic faces of monomers. In a second step, at higher concentration, the primary micelles agglomerate to form secondary micelles of larger size by hydrogen bonds between hydroxyl groups.

Mitoxantrone (1,4-dihydroxy-5,8-bis[2-(2-hydroxyethyl-amino)ethyl-amino]-anthracene-9,10-dione) is an amino-anthraquinone anticancer drug designed and synthesized to improve the clinical activity of anthracycline drugs. Mitoxantrone has shown significant clinical effectiveness in the treatment of a range of human malignancies, mostly metastatic breast cancer, lymphoma and leukemia [13, 14]. Structurally mitoxantrone is symmetrical, containing a tricyclic planar chromophore substituted with two nitrogen-containing side chains, positively charged at physiological *p*H (fig. 1).

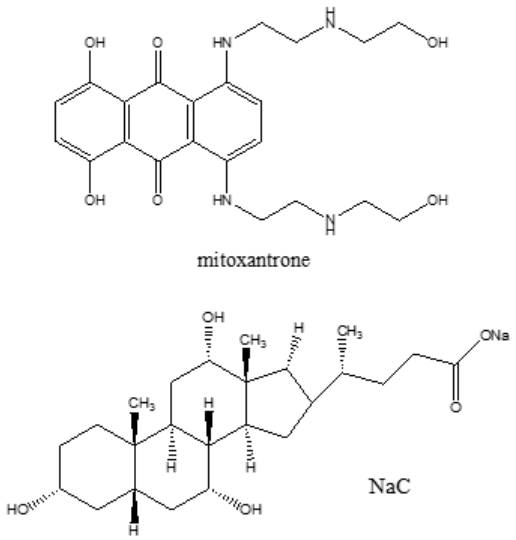

Fig. 1 Chemical structures of mitoxantrone and NaC

Different studies regarding the mechanism of mitoxantrone action indicate that nuclear DNA is the major target and the planar anthraquinone ring intercalates between DNA base pairs whereas the side groups are involved in the electrostatic binding with the negatively charged phosphate groups [15-18]. Although mitoxantrone has lower toxicity than anthracyclines, high doses of mitoxantrone or its frequent administration can produce different potential toxic effects, one of the most important side effects associated with mitoxantrone treatment being cardiotoxicity [19]. Different drug delivery systems were studied in an attempt to improve the anticancer activity of mitoxantrone and to prevent harmful side effects [20, 21]. The surfactant micelles are useful in drug delivery as they ensure the transport to specific sites of action, minimize drug degradation and loss, prevent harmful side effects

* email: enachemir@yahoo.com

and increase drug bioavailability [22]. Because biological membranes are extremely complex multicomponent structures, surfactant micelles with much less complexity have been used as model system for biomembranes to investigate the interactions of different drug molecules with biological membranes [22]. In the context of the possibility of utilization of surfactant micelles as drug carrier and deeper insights into the interaction of anticancer drugs with biological membranes, we performed a detailed physicochemical investigation on the interaction of mitoxantrone with anionic [23], cationic [24] and non-ionic [25] micelles by employing spectral and electrochemical measurements. Because of the biocompatible and biodegradable nature as well as the uniqueness of the aggregation behaviour, the bile salts micelles are very safe and efficacious drug delivery systems for medical applications and their interaction with drugs has been the subject of much interest [26, 27].

In the present work, the interaction of anticancer drug mitoxantrone with sodium cholate (NaC) bile salt has been investigated by UV-Vis absorption spectroscopy at different temperatures. The variations of mitoxantrone monomer absorption maximum in the presence of NaC were used to calculate the binding constant, stoichiometric ratio, partition coefficient of mitoxantrone between aqueous and micellar phases and the corresponding thermodynamic parameters for the above two processes.

Experimental part

Mitoxantrone dihydrochloride and NaC were analytical grade, supplied by Sigma Aldrich and used without further purification. Experiments were performed in 0.15 M sodium phosphate buffer (*p*H 7.4) and 0.15 M carbonate buffer (*p*H 10) and deionized water (18.2 MΩcm, Mili-Q water purification system) was used for the preparation of solutions. The absorption spectra of mitoxantrone were recorded in the range of 450-800 nm using a JASCO V-630 spectrophotometer equipped with the peltier-controlled ETCR-762 model accessory (JASCO Corporation, Tokyo, JP). Fresh solutions were prepared every time by subsequent dilutions from the stock. Mitoxantrone-bile salt binding constant and micelle-water partition coefficient were determined from the monomer absorbances of series of solutions containing a fixed drug concentration and increasing bile salt concentrations. In order to resolve the overlapping spectral components in the visible absorption spectra of mitoxantrone, the spectra were deconvoluted with Gaussian multi-peaks function in PeakFit 4.11 software. Linear fitting of the experimental data was performed using Origin 7.0 software.

Results and discussions

UV-Vis absorption studies

Interaction of anticancer drug mitoxantrone with NaC bile salt has been investigated by UV-Vis absorption spectroscopy in phosphate buffer (*p*H 7.4) and carbonate buffer (*p*H 10), at different temperatures. Mitoxantrone is a weakly basic drug with two ionizable amines with pKa values of 8.3–8.6 [28]. Therefore, we have studied the interaction of mitoxantrone with NaC at *p*H 7.4, when mitoxantrone exists as dication with two positive charges on the aliphatic side chains and pH 10, when mitoxantrone is uncharged due to the deprotonation of amino groups of side chains [29].

The visible absorption spectrum of mitoxantrone in phosphate buffer (*p*H 7.4) presents three overlapping spectral components: absorption maxima at 610 and 660 nm corresponding to the dimer (D) and monomer (M) of the drug and a shoulder at about 560 nm, more evident at higher drug concentration assigned to the higher aggregates (HA) of the drug [30]. In carbonate buffer (*p*H 10), the absorption maxima of dimer and monomer are red shifted and the ratio of monomer to dimer absorbances decreases indicating that dimerization process is favored in basic environment [30]. Also, at both *p*H values the position of absorption maxima of dimer and monomer does not change with temperature but the ratio of monomer to dimer absorbances increases with temperature indicating the dissociation of mitoxantrone aggregates (dimers or higher aggregates) with increasing temperatures (data not shown).

The absorption spectra of mitoxantrone in the presence of different NaC concentrations and two temperatures are shown in figure 2 for *p*H 7.4. It can be observed that after gradual addition of NaC, the absorbance of both 610 nm and 660 nm bands increases but the absorbance band at 660 nm corresponding to the drug monomer becomes predominant (spectra 7 and um 5). At the same time, the absorbance of 570 nm band corresponding to the higher aggregates of the drug decreases. Moreover, in the presence of NaC micelles a red shift of both absorbance maxima can be observed (616 and 669 nm, respectively). This red shift of the absorbance maxima may be due to the lower polarity around mitoxantrone molecules after their binding to NaC micelles and their transfer from highly polar aqueous solution to the less polar (hydrophobic) environment of bile salt micelles.

The spectral behavior of mitoxantrone in the presence of NaC at *p*H 10 is quite similar with the behavior at *p*H 7.4 (data not shown): the absorbance of monomer and dimer bands increases, the absorbance of higher aggregates band decreases and the maximum absorption bands of

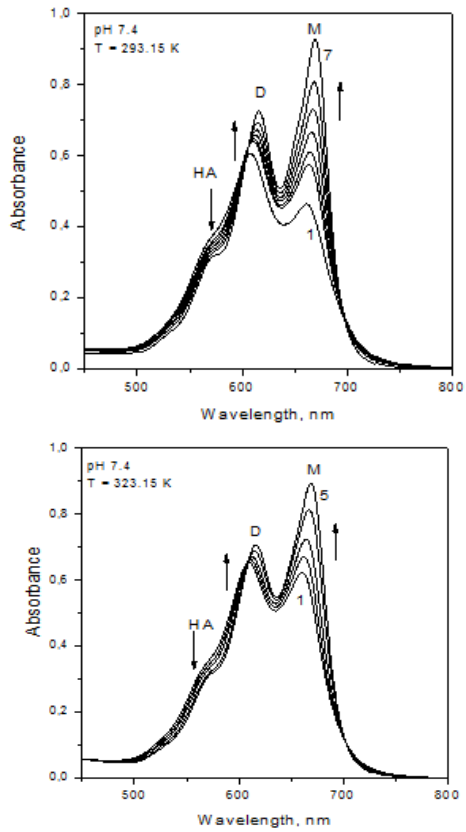

Fig. 2. Absorption spectra of mitoxantrone (2.37×10^{-5} M) in phosphate buffer *p*H 7.4 at 293.15 K and 323.15 K temperature, in the presence of different NaC concentrations: [NaC] = 0 (spectrum 1) - 1.82×10^{-2} M (spectra 7 and 5). The arrows indicate the decrease or increase of M, D and HA absorption bands.

mitoxantrone are shifted towards longer wavelengths (623 and 677 nm, respectively).

Figure 3 shows the variation of monomer, dimer and higher aggregate components with NaC concentration at *p*H 7.4 and *p*H 10, obtained from deconvolution of the spectra. It can be observed that in the absence of NaC the dimer component is constant (about 45%) at both *p*H values while the higher aggregates component increases on expense of monomers at *p*H 10 as against ***p***H 7.4. In the presence of increasing NaC concentration, at both *p*H values the monomer component is increasing up to a constant value (about 50%), on expense of dimers and higher aggregates, indicating the dissociation of these species caused by the interaction of mitoxantrone with NaC micelles (the equilibrium monomer ↔ dimer ↔ higher aggregates being shifted towards monomer formation). Also, it should be noted that for high NaC concentrations, the monomer, dimer and higher aggregate components reach the same constant values at both *p*H values.

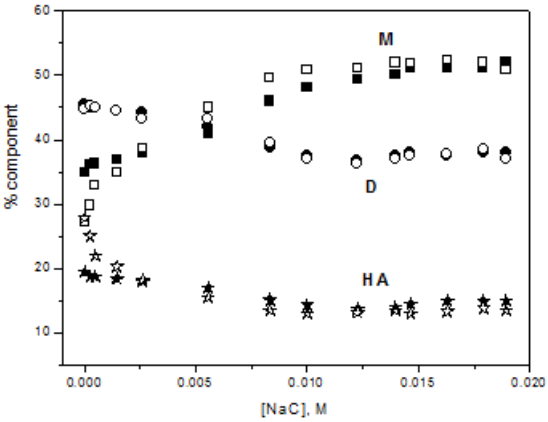

Fig. 3. Variation of the percent of component band areas in deconvoluted spectra for monomer (M), dimer (D) and higher aggregates (HA) with NaC concentration in phosphate buffer *p*H 7.4 (filled symbols) and carbonate buffer *p*H 10 (open symbols).

The variation of the monomer absorbance of mitoxantrone as a function of NaC concentration is shown in figure 4 for different temperatures and *p*H 7.4 and 10.

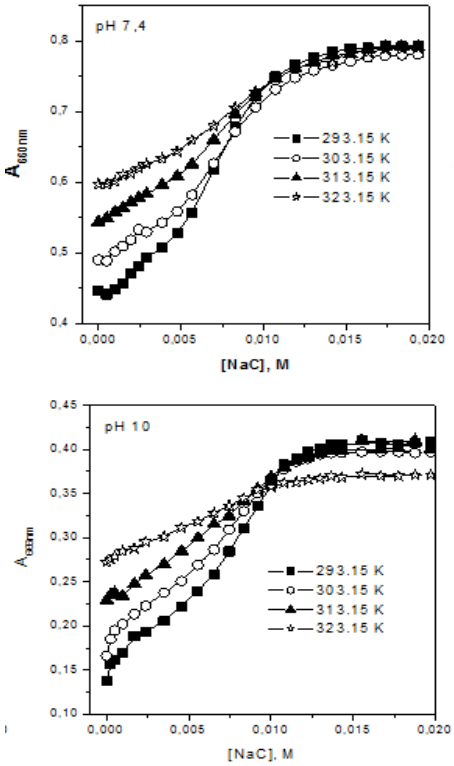

Fig. 4. Variation of the mitoxantrone absorbance at 660 nm with NaC concentration in phosphate buffer *p*H 7.4 and carbonate buffer *p*H 10, at different temperatures

For all temperatures, the monomer absorbance increases almost linearly with the concentration of NaC up to about 13 mM, which is the critical micellar concentration of NaC in 0.1 M salt solution [31]. For NaC concentrations higher than 13 mM, the monomer absorbance attains almost a constant value and it can be attributed to the complete solubilization of mitoxantrone monomers into NaC micelles. The increase in the absorbance and the progressive red shift of the absorbance maxima, even at NaC concentrations lower than CMC, indicate a strong interaction between NaC and mitoxantrone monomers, similar with the interaction of Nile Blue A with NaC [32]. For NaC concentration lower than CMC, this interaction can be attributed to the electrostatic interaction between the cationic drug molecule and the anionic bile salt monomers, similar with the interaction of mitoxantrone with anionic surfactant sodium dodecyl sulfate [23]. As against sodium dodecyl sulfate surfactant, NaC monomer has a convex hydrophobic surface with three methyl groups. Therefore, at NaC concentrations lower than CMC, mitoxantrone may bind to NaC monomers through electrostatic interaction, but in addition by hydrophobic interaction between the hydrophobic surface of NaC and the aromatic chromophore of the drug. The hydrophobic interaction dominates at higher concentration of NaC due to formation of micelles which results in encapsulation of mitoxantrone monomers in the hydrophobic cavity of bile salt aggregates. Besides the hydrophobic interaction of mitoxantrone with NaC micelles, the hydroxyl groups of the drug may form hydrogen bonding with the hydroxyl groups of NaC, which also facilities the binding of mitoxantrone in NaC micelles.

Determination of binding constant, partition coefficient and thermodynamic parameters

The variation of mitoxantrone monomer absorbance at 660 nm in the presence of NaC can be utilized to determine the binding constant of mitoxantrone to bile salt micelles and the partition coefficient of mitoxantrone between aqueous and micellar phases, and the respective thermodynamic parameters to obtain quantitative information about the interaction between mitoxantrone and NaC micelles. The binding constant (K_b) and the stoichiometric ratio (n) for mitoxantrone-NaC complexes were estimated from the Benesi-Hildebrand equation [33, 34]:

$$\frac{1}{A-A_0}=\frac{1}{K(A_1-A_0)[NaC]^n}+\frac{1}{A_1-A_0} \qquad (1)$$

where A, A_0 and A_1 are the absorbance values of mitoxantrone in presence of NaC, in absence of NaC and the absorbance due to the formation of drug-bile salt complex. The double reciprocal Benesi-Hildebrand plots of $1/(A-A_0)$ versus $1/[NaC]^n$ for all mitoxantrone-NaC complexes should be linear for the correct stoichiometry (n) [35]. The values of binding constant for mitoxantrone-NaC complexes at different temperatures are given in table 1.

As shown in figure 5, a linear Benesi-Hildebrand plot was obtained for mitoxantrone-NaC micelle binding at all investigated temperatures when n = 2 indicating a 1:2 stoichiometry for these complexes. As evident from table1, the binding constants increase with increasing temperature at both *p*H values. Thus high temperature induces stronger interactions between mitoxantrone molecules and NaC micelles. Also, the binding constants are higher at *p*H 10 than those at *p*H 7.4 for all investigated temperatures. Studies regarding the temperature influence of the bile salts

Table 1

BINDING CONSTANTS AND THERMODYNAMIC PARAMETERS FOR THE INTERACTION OF MITOXANTRONE WITH NaC IN PHOSPHATE BUFFER *p*H 7.4 AND CARBONATE BUFFER *p*H 10

pH 7.4					pH 10			
T (K)	K / 10^3 (M^{-2})	ΔG_b^0 ($kJmol^{-1}$)	ΔH_b^0 ($kJmol^{-1}$)	ΔS_b^0 ($Jmol^{-1}K^{-1}$)	K / 10^3 (M^{-2})	ΔG_b^0 ($kJmol^{-1}$)	ΔH_b^0 ($kJmol^{-1}$)	ΔS_b^0 ($Jmol^{-1}K^{-1}$)
293.15	4.36±0.11	-20.41	18.89	134.06	9.51±0.12	-22.31	12.48	118.68
303.15	6.10±0.09	-21.96		134.75	12.11±0.19	-23.68		119.28
313.15	8.29±0.13	-23.48		135.30	14.22±0.13	-24.88		119.30
323.15	8.71±0.08	-24.36		133.84	15.24±0.11	-25.86		118.64

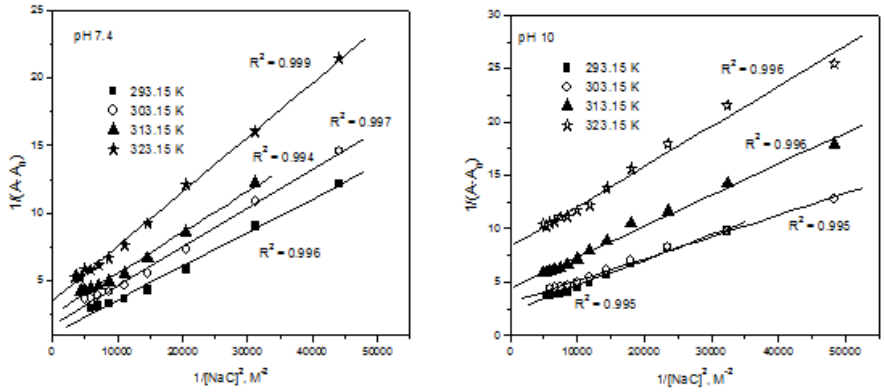

Fig. 5. Benesi-Hildebrand plots for the binding interaction of mitoxantrone with NaC micelles in phosphate buffer *p*H 7.4 and carbonate buffer *p*H 10, at different temperatures

micellization indicate that the formation of primary micelles is unaffected, while the secondary micelles tend to grow in size with increase in temperature [36]. Therefore, increasing temperature leads to the formation of fluffy micelles with less rigid interior [36] and the binding of mitoxantrone molecules is favored.

Partition coefficient (K_x) was determined from the following equation, according to the pseudo-phase model [37]:

$$\frac{1}{\Delta A} = \frac{1}{\Delta A_\infty} + \frac{n_w}{K_x \Delta A_\infty (C_T + [NaC] - CMC)} \quad (2)$$

where $\Delta A = A - A_0$, $\Delta A_\alpha = A_b - A_0$ and $n_w = 55.5$ M is the molarity of water. The value of K_x is obtained as shown in figure 6 for different temperatures. Analysis of the results from table 2 shows that mitoxantrone exhibit quite high partition coefficients for both *p*H values, indicating large scale transfer of mitoxantrone molecules from the aqueous to the micellar media. Also, the results indicate that the partition coefficient decreases with the increase in temperature for *p*H 7.4 but increases with increasing temperature for *p*H 10. Therefore, it is conclusive that mitoxantrone monomers are entrapped more efficient in NaC micelles at *p*H 7.4 and low temperature.

To evaluate the thermodynamic aspects of the binding and partitioning of mitoxantrone to NaC micelles, the thermodynamic parameters were calculated and are summarized in tables 1 and 2. The values of the Gibbs free energy of interaction (ΔG_b^0) and the Gibbs free energy of the transfer of drug from bulk aqueous phase to micellar phase (ΔG_x^0) and the corresponding standard enthalpy (ΔH^0) and the standard entropy (ΔS^0) changes were calculated from the values obtained for K_b and K_x at different temperatures from the spectral studies using the following equations:

$$\Delta G^0 = -RT \ln K \quad (3)$$

$$\Delta H^0 = \frac{\partial(\Delta G^0/T)}{\partial(1/T)} \quad (4)$$

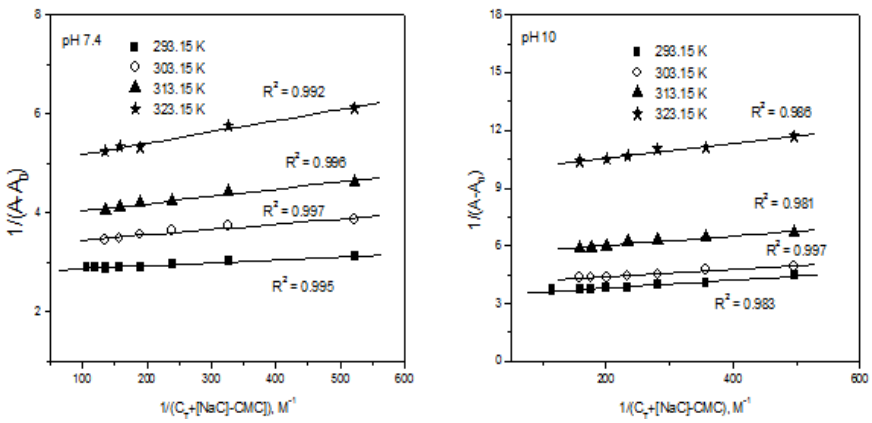

Fig. 6. Plot of $1/(A-A_0)$ versus $1/(C_T + [NaC] - CMC)$ for the interaction of mitoxantrone with NaC in phosphate buffer *p*H 7.4 and carbonate buffer *p*H 10, at different temperatures.

Table 2
PARTITION COEFFICIENTS AND THERMODYNAMIC PARAMETERS FOR THE INTERACTION OF MITOXANTRONE WITH NaC IN PHOSPHATE BUFFER *p*H 7.4 AND CARBONATE BUFFER *p*H 10

	pH 7.4				pH 10			
T (K)	K_x / 10^5	ΔG_x^0 (kJmol^{-1})	ΔH_x^0 (kJmol^{-1})	ΔS_x^0 (Jmol^{-1}K^{-1})	K_x / 10^5	ΔG_x^0 (kJmol^{-1})	ΔH_x^0 (kJmol^{-1})	ΔS_x^0 (Jmol^{-1}K^{-1})
293.15	2.61±0.08	-30.38	-20.00	35.41	0.89±0.05	-27.76	12.01	-135.66
303.15	1.85±0.03	-30.55		34.80	1.17±0.04	-29.40		-136.60
313.15	1.49±0.01	-31.00		35.13	1.28±0.06	-30.60		-136.07
323.15	1.20±0.02	-31.41		35.31	1.43±0.01	-31.88		-135.82

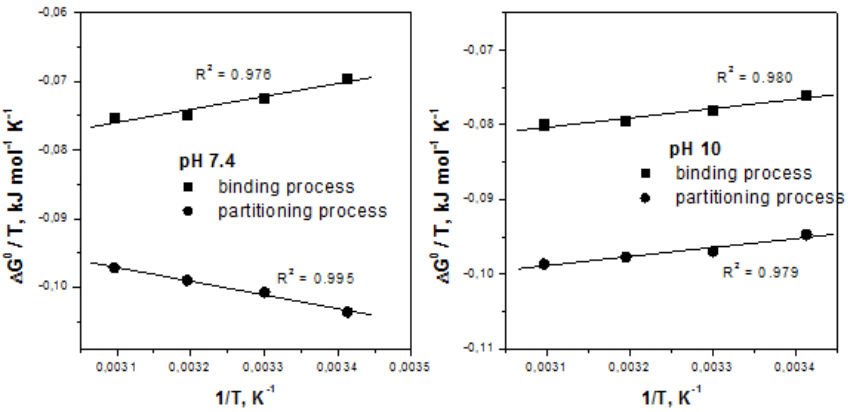

Fig. 7. Plot of DG^0/T versus 1/T for the binding and partition of mitoxantrone to NaC micelles in phosphate buffer *p*H 7.4 and carbonate buffer *p*H 10

$$\Delta S^0 = \frac{\Delta H^0 - \Delta G^0}{T} \quad (5)$$

According to eq. (4), a plot of $\Delta G^0/T$ versus 1/T gives a straight line and the slope of this line is equal with ΔH^0 (fig. 7).

As seen from tables 1 and 2, ΔG^0 values are negative at each investigated temperature for both binding and partitioning processes of mitoxantrone to NaC micelles, indicating about the spontaneity of both processes. Moreover, with increase in temperature the ΔG^0 values become more negative for both processes at both *p*H values. This means that binding and partitioning of mitoxantrone to NaC micelles are highly spontaneous at higher temperatures. The positive values of ΔH^0 indicate that the binding process is endothermic at both *p*H values, while the partitioning process is exothermic at *p*H 7.4 and endothermic at *p*H 10. The positive values of ΔS_b^0 and ΔH_b^0 indicate that the binding process of mitoxantrone to NaC micelles is entropy controlled over the range of studied temperatures, at both *p*H values. Also, the positive values of ΔS_b^0 and ΔH_b^0 indicate that the interaction of mitoxantrone with NaC micelles is mainly hydrophobic. The positive values of ΔS_b^0 are higher for the interaction of mitoxantrone with NaC micelles at *p*H 7.4 than that for *p*H 10 and could reflect a more pronounced hydrophobic interaction. In the case of partition process of mitoxantrone between micellar and bulk aqueous phases, the entropy values are positive at *p*H 7.4 but negative at *p*H 10. Therefore, the partitioning process is entropy controlled at *p*H 7.4 and enthalpy controlled at *p*H 10.

Conclusions

In view of the importance of fundamental knowledge about the interaction of a drug with bile salts, we have investigated in this paper the interaction of anticancer drug mitoxantrone with NaC (a trihydroxy bile salt) in phosphate buffer (*p*H 7.4) and carbonate buffer (*p*H 10) by following the changes in the absorption spectra of drug molecule as a function of bile salt concentration and as a function of temperature. The results indicated that mitoxantrone may bind to NaC monomers and micelles through electrostatic and hydrophobic interactions and the interaction with NaC induces the dissociation of dimers and higher aggregates of mitoxantrone. The ΔG^0 values indicate that binding and partitioning of mitoxantrone to NaC micelles are highly spontaneous at higher temperatures at both *p*H values. The positive values of ΔS_b^0 and ΔH_b^0 are indicative of enhanced hydrophobic interactions between hydrophobic chromophore of mitoxantrone and hydrophobic surface of NaC, the binding process being entropy controlled over the range of studied temperatures, at both *p*H values. The partition process of mitoxantrone between micellar and bulk aqueous phases is entropy controlled at *p*H 7.4 and enthalpy controlled at *p*H 10.

References

1. MALDONADO-VALDERRAMA, J., WILDE, P., MACIERZANKA, A., MACKIE, A., Adv. Colloid Interface Sci., **165,** 2011, p. 36.
2. HOLM, R., MULLERTZB, A., MU, H., Int. J. Pharm.**,** **453**, 2013, p. 44.
3. CHEN, Y.P., LU, Y., CHEN, J.M., LAI, J., SUN, J., HU, F.Q., WU, W., Int. J. Pharm.**,** **376**, 2009, p.153.
4. ZHANG, Y., DENG, Y.J., LU, M., DUNCAN, Q.M.C., LI, Z.Q., J. Colloid Interface Sci., **337**, 2009, p. 322.
5. MADENCI, D., EGELHAAF, S.U., Curr. Opin. Colloid Interface Sci., **15**, 2010, p. 109.
6. THAKUR, R., DAS, A., ADHIKARI, C., CHAKRABORTY, A., Phys. Chem. Chem. Phys., **14**, 2012, p. 15369.
7. AMUNDSON, L.L., LI, R., BOHNE, C., Langmuir, **24**, 2008, p. 8491.

8. MANDAL, S., GHOSH, S., BANIK, D., BANERJEE, C., KUCHLYAN, J., SARKAR, N., J. Phys. Chem. B, **117**, 2013, p. 13795.
9. MANDAL, S., GHOSH, S., BANERJEE, C., RAO, V.G., SARKAR, N., J. Phys. Chem. B, **116**, 2012, p. 8780.
10. SMALL, D.M. in Adv. Chem. Ser. (Ed. E.D. Goddard) **1968**, Vol. 84, Ch. 4, pp. 31-42 (New York: Plenum Press).
11. CAREY, M.C., SMALL, D.M., J. Colloid Interface Sci., **31**, 1969, p. 382.
12. SMALL, D.M., PENKETT, S.A., CHAPMAN, D., Biochim. Biophys. Acta, **176**, 1969, p. 178.
13. CARMO-PEREIRA, J., OLIVEIRA COSTA, F., HENRIQUES, E., Eur. J. Cancer, **29**, 1993, p. 1814.
14. SHENKENBERG, T.D., VON HOFF, D.D., Ann. Intern. Med., **105**, 1986, p. 67.
15. LI, N., MA, Y., YANG, C., GUO, L., YANG, X., Biophys. Chem., **116**, 2005, p. 199.
16. AGARWAL, S., JANGIR, D.K., MEHROTRA, R., J. Photochem. Photobiol. B, **120**, 2013, p. 177.
17. ENACHE, M., VOLANSCHI, E., Rev. Roumaine Chim., **50**, 2005, p. 131.
18. HAJIHASSAN, Z., RABBANI-CHADEGANI, A., Int. J. Biol. Macromol., **48**, 2011, p. 87.
19. MURRAY, T.J., Expert Opin. Drug Saf., **5**, 2006, p. 265.
20. MA, Y., ZHOU, L., ZHENG, H., XING, L., LI, C., CUI, J., CHE, S., J. Mater. Chem., **21**, 2011, p. 9483.
21. LI, C., CUI, J., WANG, C., WANG, J., LI, Y., ZHANG, L., ZHANG, L., GUO, W., WANG, Y., Int. J. Pharm., **362**, 2008, p. 60.
22. RANGEL-YAGUI, C.O., PESSOA-JR, A., TAVARES. L.C., J. Pharm. Pharmaceut. Sci., **8**, 2005, p. 147.
23. ENACHE, M., ANGHELACHE, I., VOLANSCHI, E., Int. J. Pharm., **390**, 2010, p. 100.
24. ENACHE, M., VOLANSCHI, E., J. Pharm. Sci., **100**, 2011, p. 558.
25. ENACHE, M., VOLANSCHI, E., J. Pharm. Pharmacol., **64**, 2012, p. 688.
26. NATALINI, B., SARDELLA, R., GIOIELLO, A., IANNI, F., DI MICHELE, A., MARINOZZI, M., J. Pharm. Biomed. Anal., **87**, 2014, p. 62.
27. MAHAJAN, S., MAHAJAN, R.K., J. Colloid Interface Sci., **387**, 2012, p. 194.
28. RAGHUNAND, N., MAHONEY, B.P., GILLIES, R.J., Biochem. Pharmacol., **66**, 2003, p. 1219.
29. FEOFANOV, A., SHARONOV, S., KUDELINA, I., FLEURY, F., NABIEV, I., Biophys. J., **73**, 1997, p. 3317.
30. ENACHE, M., VOLANSCHI, E., Rev. Roum. Chim., **55**, 2010, p. 255.
31. WIEDMANN, T.S., KAMEL, L., J. Pharm. Sci., **91**, 2002, p. 1743.
32. MISHRA, S.S., SUBUDDHI, U., J. Colloid Photochem. Photobiol. B, **141**, 2014, p. 67.
33. BENESI, H.A., HILDEBRAND, J.H., J. Am. Chem. Soc., **71**, 1949, p. 2703.
34. SHIRAISHI, Y., SUMIYA, S., KOHNO, Y., HIRAI, T., J. Org. Chem., **73**, 2008, p. 8571.
35. SUBUDDHI, U., MISHRA, A.K., Colloids Surf. B, **57**, 2007, p. 102.
36. SUGIOKA, H., MATSUOKA, K., MOROI, Y., J. Colloid Interface Sci., **259**, 2003, p. 156.
37. KAWAMURA, H., MANABE, M., MIYAMOTO, Y., FUJITA, Y., TOKUNAGA, S., J. Phys. Chem., **93**, 1989, p. 5536.

Manuscript received: 15.07.2017